SPE SA (0526)

Estimating the Amount of free Sand in the Yielded Zone around Vertical and Horizontal Oil Wells

Musaed N. J. Al-Awad and Talal Y. Al-Ahaidib, King Saud University, College of Engioneering, Petroleum Engineering Department

This paper was prepared for presentation at the 2005 SPE Technical Symposium of Saudi Arabia Section held in Dhahran, Saudi Arabia, 14-16 May 2005.

Abstract

Predicting sand production accurately is a difficult task; many techniques have been previously investigated such as production history, mechanical property analysis using electrical log data, laboratory testing and computer modeling.

In this study, the mechanism of sand production problem in an oil reservoir producing medium oil (30^o API) from a weak sandstone formation was investigated. An analytical model is elaborated based on linear-poroelastic solution of stress state around circular openings as well as Mohr-Coulomb failure criterion and Darcy's equations for fluid flow through porous media in vertical and horizontal wellbores.

In this study, a new important factor necessary for the estimation of the mount of free sand generated between sheared planes caused by the fluid drawdown was introduced. This factor is called sand production capability factor. Sand capability factor was evaluated experimentally for the studied reservoir.

Observations of sand production in the studied oil reservoir were utilized to tune and verify the model used in this study. For open-hole completion, it was found that; free sand ready to move into the wellbore is inversely proportional to radial distance. Furthermore, free sand ready for production from the yielded zone around vertical wells is higher than that in the case of horizontal wells. The predicted free sand in all studied cases is in accordance with field observations.

Selection of borehole and perforation orientation (in case of perforated casing completion) with respect to the maximum horizontal principal in-situ stress has a great effect in reducing the potential free sand amounts ready to move into the wellbore along with the producing reservoir fluids. Horizontal wellbores oriented at 45^o produce minimum sand compared with other horizontal orientations for the studied reservoir. Similar effect is found for perforations phased at zero angular position.

Introduction

Sand production can be defined as the production of sand grains detached from the reservoir sandstone formation along with the produced hydrocarbon to the surface. Sand production is an exceedingly complex problem, which has troubled the oil industry worldwide. Every year, the petroleum industry spends millions of dollars on cleaning out sand from wells and repairing problems associated with the sand production such as borehole instability, casing collapse, wear of downhole and surface equipment, etc. As a result, tremendous production quantities are lost or deferred. Sand production from highly unconsolidated sandstone reservoirs can occur as soon as the well is brought on production. In more consolidated reservoirs, sand production may occur for short periods of time followed by periods of sand-free production that varies from well to well and from reservoir to reservoir. Sand production and its associated erosion and plugging of equipment also represent a potential safety hazard. Subsequently, huge investments are made in many oil and gas fields worldwide to prevent sand from being produced to the surface [1-16].

Elaboration of the Mathematical Model

Solution for Stresses around Circular Openings

Linear-poroelastic solution for stresses around circular openings (Kirch solution) is a method used to compute the redistributed (induced) stresses around a circular borehole caused by the removal of drilled rocks. This solution assumes that the studied formation is porous, homogeneous, isotropic and linear-elastic. This allows the production-induced stresses (σ_r, σ_θ, σ_{zz} and $\tau_{\theta z}$) to be determined from a set of fairly simple equations [15].

To ably the above model for oil production case, it is necessary to transform the principal in-situ stresses (σ_v, σ_H and σ_h) acting of the reservoir under study into the axis of the borehole in case of deviated and horizontal wells. The in-situ stresses in the case of deviated or horizontal wells can be transformed to the direction of the well axis by the application of a set of equations derived based on the geometry shown **Fig. 1** [17, 18]:

By introducing the principle of effective stress (i.e. subtracting the effect of pore fluid pressure (Pp)) and accounting for Biot's constant effect (β_c), the major and minor induced effective stresses acting on the formation under consideration are the maximum and minimum values of the three induced stresses computed using the following equations [17, 18]:

$$\sigma_1 = \sigma_r - \beta_c P_p \quad \ldots(1)$$

$$\sigma_2 = \frac{1}{2}(\sigma_\theta + \sigma_z) - \frac{1}{2}\sqrt{(\sigma_\theta - \sigma_z)^2 + 4\tau_{\theta z}} - \beta_c P_p \quad \ldots(2)$$

$$\sigma_3 = \frac{1}{2}(\sigma_\theta + \sigma_z) + \frac{1}{2}\sqrt{(\sigma_\theta - \sigma_z)^2 + 4\tau_{\theta z}} - \beta_c P_p \quad \ldots(3)$$

Mohr-Coulomb Failure Criterion

Mohr-Coulomb failure or strength criterion has been widely used for geotechnical applications. Mohr-Coulomb criterion assumes that failure is controlled by the maximum shear stress and that this failure shear stress depends on the acting normal stress. This can be represented by plotting Mohr circles for the states of stress at each failure (test) in terms of the maximum and minimum principal stresses (σ_1 and σ_2 or σ_3). The Mohr-Coulomb failure line (envelope) is the best straight line that touches these Mohr circles. Thus, Mohr-Coulomb criterion can be written as follows [17]:

$$|\tau_f| = \tau_o \pm \sigma_f \tan\phi \quad \ldots(4)$$

Shear (τ_f) and effective normal (σ_f) components of the stress acting on the plan inclined at an angle ϕ with the direction of the maximum principal stress (σ_1) are shown in **Fig. 2**.

A Mohr-Coulomb failure criterion for a specific material is established by carrying out triaxial tests on cylindrical core samples at various confining pressures; axial stresses at failure are recorded. From this data, a series of Mohr circles can be plotted. A common tangent for these circles can be drawn which defines the failure envelope. The tangent line gives the value of the angle of internal friction (ϕ) and the intercept with the shear stress axis gives the value of the apparent cohesion (τ_o). Any data point lies above the failure envelope is considered to be in unstable state.

Darcy’s Equations for Fluid Flow in Porous Media

Darcy’s law for radial fluid flow into vertical wells can be written as follows [19]:

$$Q_V = \frac{7.081\, k\, h\, \Delta P}{\mu \beta_o \ln\left(\frac{r_e}{r_w}\right)} \quad \ldots(5)$$

Similarly, Darcy’s law for radial fluid flow into horizontal wells can be written as follows [20]:

$$Q_H = \frac{7.081\, k\, h\, \Delta P}{\mu \beta_o \left[\ln\left(\frac{1+\sqrt{1-\left(\frac{L}{2 r_e}\right)^2}}{\left(\frac{L}{2 r_e}\right)}\right) + \left(\frac{h}{L}\right)\ln\left(\frac{h}{2\pi r_w}\right)\right]} \quad \ldots(6)$$

Using Eqs. 5 and 6, pressure drop in the wellbore can be calculated if the production rate is known.

The Average Sand Production Capability Factor

Sand production problem is usually encountered when producing oil from moderately strong or weak sandstone reservoirs. The produced sand is generated due to frictional action on the induced microfractures concentrated in the yielded zone around the borehole caused by excessive oil drawdown. In a previous study [10], a single constant value was designated for sand production capability factor (C_a). This assumption is incorrect, because it either overestimates or underestimates the amounts of free sand in the yielded zone around boreholes or perforations ready to move into the wellbore. The amount of generated free sand varies with radial distance, i.e. sand amount is maximum near the wellbore face and approaches zero as we reach the intact formation few inches away from the wellbore. This assumption is based on the fact that higher induced stresses are concentrated on the formation at the wellbore face. Average sand production capability factor is experimentally evaluated for the studied reservoir.

In evaluating sand production capability factor, cylindrical core samples from the reservoir under study are tested. These samples are mounted into Hoek cell and a specific confining pressure is applied. Axial load is gradually increased until failure is observed then the test is terminated at this stage. The samples are carefully extracted from the cell and the generated sand is collected. At each confining pressure, two samples are tested and the average free sand volume is calculated. The Average sand production capability factor at any confining pressure is calculated by relating the volume of the generated free sand after failure to the initial volume of the sample before failure. Similarly, the above steps are repeated for several confining pressure values. Finally, a correlation is obtained by plotting sand production capability factor (C_a) versus confining pressure values as follows (see **Fig. 3**):

$$C_a = 0.79992 - 1.0863 * 10^{-3}(\sigma_3) + 6.7118 * 10^{-7}(\sigma_3)^2 - 2.063 * 10^{-10}(\sigma_3)^3 + 3.1141 * 10^{-14}(\sigma_3)^4 - 1.8413 * 10^{-18}(\sigma_3)^5 \quad \ldots(7)$$

For comparison, three single values for the sand production capability factor were also plotted in the same graph indicating the maximum (at the face of the wellbore), minimum (near the intact rock) and the average values for this factor. It is well known that the stability of the formation rock increases with the increase in the natural horizontal confining support (σ_3) provided by the adjacent rock as moving away from the wellbore, which is assumed to be equivalent to the laboratory, applied confining pressure. This correlation is used in the elaborated model to estimate sand amount ready to move with the produced fluids as a function of radial distance.

Sand Production Prediction Technique

All previous studies [1-11, 13-16] predict the onset of sand production based on the assumption that failure occurs only on the wellbore face and neglect the state of rock far from the wellbore. Furthermore, these studies were not able to predict the amount of free sand generated due to rock yielding caused by production induced stresses. In this study, the elaborated model searches for failure (yielding) starting from the face of the borehole and deeper into the formation until intact rock is reached.

The systematic steps used by the above mentioned model to predict the onset of free sand generation in the yielded zone around boreholes or perforations are as follows:

Step 1:
Reservoir properties data such as permeability, viscosity of produced fluid, radius of drainage area, plus rock mechanical properties data such as Poisson's ratio, apparent cohesion, along with other data such as maximum and minimum horizontal in-situ principal stresses, vertical in-situ principal stress, inclination, orientation and azimuth angles, formation thickness, and production rate, are required as an input parameters.

Step 2:
Accordingly the model transforms the principal in-situ stresses (σ_v, σ_H and σ_h) into the direction of the wellbore and calculates the production induced stresses (σ_r, σ_θ and σ_{zz}).

Step 3:
By comparison, the values of the principal induced stresses (σ_1 and σ_3) acting on the productive formation around the wellbore or perforations are found and then transformed into effective stresses.

Step 4:
Once the principal induced stresses mentioned in the previous step are determined, the model calculates and compares shear stresses: firstly production induced shear stress $(\tau_f)_P$ and maximum allowable shear stress (based on laboratory measurements) $(\tau_f)_L$ as follows:

$$(\sigma_f)_P = \left(\frac{\sigma_1 + \sigma_3}{2}\right) - \left(\frac{\sigma_1 - \sigma_3}{2}\right) \mathrm{Cos}(2\lambda) \qquad \ldots(8)$$

$$(\tau_f)_P = \left(\frac{\sigma_1 - \sigma_3}{2}\right) \mathrm{Sin}(2\lambda) \qquad \ldots(9)$$

$$(\tau_f)_L = \tau_o + (\sigma_f)_P \,\mathrm{Tan}(\phi) \qquad \ldots(10)$$

$$\lambda = 45° + \frac{\phi}{2} \qquad \ldots(11)$$

Step 5:
A) If $(\tau_f)_P$ is greater than or equal to $(\tau_f)_L$ this will lead to an unsafe case, i.e. the possibility of sand production does exist. In this case the model calculates the possible volume of free sand and repeats the entire process starting with another radial distance away from the borehole wall and deeper into the formation until it reaches a no-failure zone (intact formation).

B) If $(\tau_f)_P$ is less than $(\tau_f)_L$ this indicates a safe case, i.e. the possibility of sand production does not exist.

Step 6:
When sand production from perforations is to be predicted, a single perforation is assumed to be equivalent to a single horizontal wellbore with dimensions corresponds to the dimensions of the perforation. The total amount of free sand then is calculated by multiplying the predicted amount of free sand generated around a single perforation by the total number of perforations communicating the wellbore with the reservoir (i.e. perforation density).

Therefore, the above set of equation can be used to predict the onset of rock yielding and potential free sand debris generated due to yielding in vertical and horizontal wells. The above procedure was applied using field as well as laboratory-derived data for an oil reservoir as shown in **Table. 1**.

Results and Discusion

Sand Movement from Formation to Surface

The movement of sand debris from the yielded formation into the wellbore occurs when drag forces of the produced fluid exceed the body forces holding the detached sand in place (i.e. between shear surfaces). At higher production rates (i.e. turbulent conditions) field experience has shown that most of the generated sand in the failed formation is moved readily into the wellbore as shown in **Fig. 4** [16]. Because the production rates in the near-wellbore region normally applied by oil companies are within the turbulent flow regime that produces drag forces high enough to move the detached sand grain from the formation to the wellbore. Once the free sand is moved into the wellbore, it could be either move up to the surface or settle down in the bottom of the well until work-over job is performed. Based on the simple Stock's formulas [21], **Fig. 5** shows the uplift velocity of a wide range of formation sand as a function of production rate. The grain size distribution of sand in the studied reservoir is shown in **Fig. 6**.

Prediction of Free Sand in the Yielded Zone

Open-hole Completion Case

Figure 7 shows the relationship between the maximum allowable and production induced (model predicted) shear stresses acting around vertical (α=0°) open-hole wellbore as a function of radial distance for the studied reservoir. It is clear that the yield zone around this borehole extend for 1.16 and 1.72 non-dimensional radii into the formation at angular positions of 0^o and 90^o respectively at 5000 bbl/day/well. The full shape (0^o-360^o) of the yielded zone around the above-mentioned vertical wellbore is shown in **Fig. 8**. Using sand production capability factor equation presented previously (Eq. 7) and the thickness of the yielded zone around the wellbore, the free sand in the yielded zone ready to move into the wellbore is calculated using the following relationship:

$$(V_s)_{total} = \Sigma\left(\pi\left(r_i^2 - r_{i-1}^2\right) h \,(C_a)_{r_i}\right) \qquad ...(12)$$

For the vertical wellbore case mentioned above, the amount of free sand in the yielded zone ready to move into the wellbore is 8.2 cubic foot that corresponds to 6.78 PTB (pound per thousand barrels) based on 5000 bbl/day production rate.

In the same manner, the relationship between the maximum allowable and model predicted shear stresses acting around horizontal open-hole completed wells as a function of radial distance for the studied reservoir at three different horizontal wellbore orientations (0^o, 45^o and 90^o) with respect to the maximum principal in-situ horizontal stress (σ_H) and the full shape of the yielded zones around those horizontal wellbores can be predicted as shown in **Figs. 9** to **14**. The predicted free sand ready to produce for these cases was 9.63, 7.46 and 12.1 cubic foot corresponding to 7.95, 6.2 and 9.92 PTB and non-dimensional radial distance of 1.53, 1.43 and 2.07 respectively. These predictions correspond with field observation [16] for the same reservoir as shown in **Fig. 5**. It is clear that, sand production from a horizontal well oriented at 45^o is the minimum among other horizontal orientations as well as vertical well case in addition to the high production rate at low drawdown pressure expected from horizontal wells in the studied reservoir.

Perforated Casing Completion Case

In perforated casing completion mode, the amount of free sand in the yielded zones generated around perforation tunnels is function of perforation length, radius and density or shoot/foot (SPF). It must be noticed that perforations in both vertical and horizontal wells are assumed to be on the sides of the well (i.e. normal to the wellbore axis). **Fig. 15** represents the relationship between perforation density, orientation with respect to the maximum horizontal principal in-situ stress and free sand volume ready to move into the wellbore. As seen in **Fig. 15**, free sand is much lower in the case of perforated casing completion when compared to open-hole completion and is highly dependent on the orientation and the density of perforations.

Effect of Sand Production Capability Factor Type

As mentioned previously, the first attempt to introduce this factor was as a constant value [12]. **Table 2** shows a comparison between results obtained based on the application of single and variable values for the sand production capability factor introduced by this study (see **Fig. 3**). It can be shown that higher amounts of free sand will be predicted when applying a single value sand production capability factor (maximum value = 0.8, average valure = 0.45 and minimum value = 0.10). Using the variable sand capability factor (Eq. 7) the estimated values of free sand are much lower than those predicted if a single value is designated for the sand production capability factor.

Conclusions

Based on the analysis performed in this study, the following conclusions are drawn:

1. A method for determining the yielded zone radius and the volume of free sand ready to produce has been elaborated based on Darcy's law, Kirch solution for linear poroelastic materials and Mohr-Coulomb failure criterion.

2. The current model provides the radial depth of the yielded formation and the amounts of free sand trapped between shear surfaces. Unfortunately, it is not possible to predict the length of time duration that is needed for this trapped sand to move into the borehole.

3. Sand debris produced due to shear failure mode is evaluated at laboratory. Thus, sand production capability factor as a function of confining stress is established for the studied reservoir.

4. For both open-hole and perforated casing completions, vertical wells produce higher sand volumes than horizontal wells, thus open-hole completion is not recommended for wells drilled in this reservoir.

5. Sand production can be minimized when oriented wellbores and oriented perforations are performed. For the studied reservoir, horizontal wells at 45^o orientation with respect to the minimum horizontal principal in-situ stress and perforation phased at zero degree angular position providing the minimal amounts of sand debris for the studied reservoir.

Nomenclature

C_a	= Sand production capability factor, dimensionless.
h	= Formation thickness, ft.
k	= Formation permeability, Darcy.
L	= Horizontal well displacement, ft.
PTB	= Sand production, pound per 1000 barrel.
P_w	= Wellbore pressure, psi.
P_p	= Formation pore fluid pressure, psi.
Q_v	= Production rate from vertical well, bbl/day.
Q_H	= Production rate from horizontal well, bbl/day.
r	= Radial distance into the formation, ft.
r_e	= Radius of the drainage area, ft.
r_w	= Wellbore radius, ft.
SPF	= Number of shoots per foot.
V	= Free sand volume in the yielded zone, ft^3.
α	= Borehole inclination (relative to vertical), degree.
β	= Borehole orientation (relative to azimuth), degree.
βo	= Formation volume factor, BBL/STB.

βc = Biot's constant, dimensionless.
ΔP = Pressure drawdown, psi.
θ = Angular position around the borehole, degree.
2λ = Angle of obliquity (failure), degree.
μ = Fluid viscosity, cp.
σ_f = Normal (total) stress, psi.
σ_1 = Max. induced stress (equivalent to axial stress), psi.
σ_3 = Min. induced stress (confining stress equivalent), psi.
$(\tau_f)_p$ = Shear stress based on experimental data, psi.
$(\tau_f)_L$ = Shear stress based on model calculations, psi.
$(\sigma_f)_L$ = Normal stress based on model calculations, psi.
σ_H = Maximum horizontal in-situ principal stress, psi.
σ_h = Minimum horizontal in-situ principal stress, psi.
σ_v = Vertical in-situ principal stress, psi.
σ_r, σ_θ, σ_{zz} = Induced stresses, psi.
τ_f = Absolute value of shear stress, psi.
τ_o = Apparent (inherent) cohesion of the material, psi.
$\tau_{\theta z}$ = Induced tangrhtial shear stress, psi.
ϕ = Angle of internal friction, degree.

References

[1] Stein, A. and Hilchie, D. W.: "Estimating the Maximum Production Rate Possible from Friable Sandstones without Using Sand Control" JPT (Sep. 1972) pp. 1157-1160.

[2] Bratli, R.K., and Risnes, R.: "Stability and Failure of Sand Arches" SPEJ, April 1981, pp. 236-248.

[3] Geertsma, J.: "Some Rock-Mechanical Aspects of Oil and Gas Well Completions" SPEJ, Dec. 1985, pp. 848-856.

[5] Morita, N. et al.: "Parametric Study of Sand-Production Prediction: Analytical Approach"SPE Production Engineering, Feb. 1989, pp. 25-33.

[6] Tronvoll, J. and Halleck, P. M.: "Observations of Sand Production and Perforation Cleanup in a Weak Sandstone." Int. J. Rock mech. Min. Sci. & Geomech. Abstr., 1994.

[7] Al-Qahtani, A. M.: "Sand Production Control: Theory and Practice, Zuluf Field," paper presented at the SPE , Dahran, Saudi Arabia, October, 1998.

[8] McLellan, P.J, Hawkes, C.D.: "Sand Production Prediction for Horizontal Wells in Gas Storage Reservoirs," paper SPE 65510 presented at the SPE/Petroleum Society of CIM International Conference, Calgary, Alberta, Canada, 2000.

[9] Wang, Y., Tremblay, B.: "Enhanced Production in Horizontal Wells by the Cavity Failure Well Completion," SPE Paper no. 68835 Presented at the SPE Western Regional Meeting, Bakersfield, CA, 26-30 march, 2001.

[10] Kooijman, A. P., Van den Hoek, P. J., Ph. De Bree, Kenter, C. J., Zheng, Z. And Khodaverdian, M.: "Horizontal Wellbore Stability and Sand Production in Weakly Consolidated Sandstones.", SPE Paper no. 36419 Presented in the SPE Annual Technical Conference and Exhibition held in Denver, USA, October 6-9, 1996, pp. 35-48.

[11] Mike, T., Juan, T. and John, L.C.: "Integrated Approach to Sand Control Delivers Zero Sand.", SPE Paper no. 81034 Presented in the SPE Latin American Petroleum Engineering conference held in Port-of-Spain, Trinidad, West Indies, April 27-30, 2003, pp. 1-7.

[12] Musaed N. J. Al-Awad, and Saad El-Din M. Desouky: "Prediction of Sand Production from a Saudi Sandstone Reservoir.", Oil & Gas Science and Technology – Revue de l'IFP, Vol. 52, No. 4, pp. 1-8, July-August, 1997.

[13] Musaed N. J. Al-Awad: "The Mechanism of Sand Production Caused by Pore Pressure Fluctuation." Oil & Gas Science and Technology Journal – Revue de l'IFP, pp. 339-345 , Vol. 56, No. 4, 2001.

[14] Veeken, C.A.M., et al.: "Sand Production Prediction Review: Developing an Integrated Approach," paper SPE 22792, Oct 1991.

[15] Oshita, T., et al.: "Integrated Approach for Sand Management: Field Application to an Offshore Oil Field," paper SPE 37767 presented at the Middle East Oil Show, Manama, Bahrain, 15-18 march, 1997.

[16] Al-Qahtani, A.M.: "Sand Production Control: Theory and Practice, Zuluf Field," paper presented at the SPE, Dhahran, Saudi Arabia, October, 1998.

[17] Erling, F. et al, "Petroleum Related Rock Mechanics", Amsterdam: Elsevier Science Publishers B.V, 1992.

[18] McLean, M. A. and Addis, M. A.: "Wellbore Stability: The Effect of Strength Criteria on Mud Weight Recommendations.", SPE Paper 20405 Presented in the65th Annual Technical Conference and Exhibition, New Orleans, USA, September 23-26, 1990, pp. 9-17.

[19] Craft, B.C. and Hawkins, M.F.: "Applied Petroleum Reservoirs.", Pretice- Hall Inc., Englewood cliffs, N.J, 1959, P437.

[20] Mukherjee, H., Economides, M.: "A Parametric Comparison of Horizontal and Vertical Well Performance," paper SPE 18303, June 2001.

[21] "Drilling Mud and Cement Slurry Rheology Manual" Edition Technip, Paris, 1982 Ed., P107.

Table 1 Raw data used to validate the elaborated model.

Formation depth = 5546.4 ft
Formation thickness = 64.7 ft
Poisson's ratio = 0.21
Uniaxial compressive strength = 1703.8 psi
Apparent cohesion = 4638 psi
Angle of internal friction = 16.5 degree
Porosity = 31.1%
Permeability = 2.1943 Darcy
Oil viscosity = 3.7 cp
Pore pressure = 2594 psi
Oil formation volume factor (βo) = 1.1 Bbl/STB
Wellbore radius (r_w) = 0.375 ft
Reservoir drainage radius (r_e) = 912 ft
Sand grain density = 165.4 pcf
Biot's constant = 0. 96
Actual (field) production rate with no continuous sand production = 5000 bbl/day
Vertical principal in-situ stress (σ_v) = 1.0 psi/ft.
Maximum horizontal principal in-situ stress (σ_H) = 1.1 psi/ft
Minimum horizontal principal in-situ stress (σ_h) = 0.71 psi/ft
h/L = 0.0741
Perforation radius = 0.33 inch
Perforation length = 14 inch

Table 2 Sand production capability factor values for open-hole completed vertical and horizontal wellbores in the studied reservoir.

Sand production capability factor, (C_a) (See **Fig. 3**)			Free sand generated in the yielded zone, ft^3			
			Vertical well ($\alpha = 0^o$ and $\theta = 0^o$-360^o)	Horizontal well ($\alpha = 90^o$ and $\theta = 0^o$-360^o)		
				$\beta = 0^o$	$\beta = 45^o$	$\beta = 90^o$
Single value	Maximum	0.80	28.32	25.50	21.20	55.80
	Average	0.45	15.83	14.40	11.90	31.40
	Minimum	0.10	3.52	3.20	2.65	6.98
Variable value	See Eq. 7		8.20	9.63	7.46	12.10

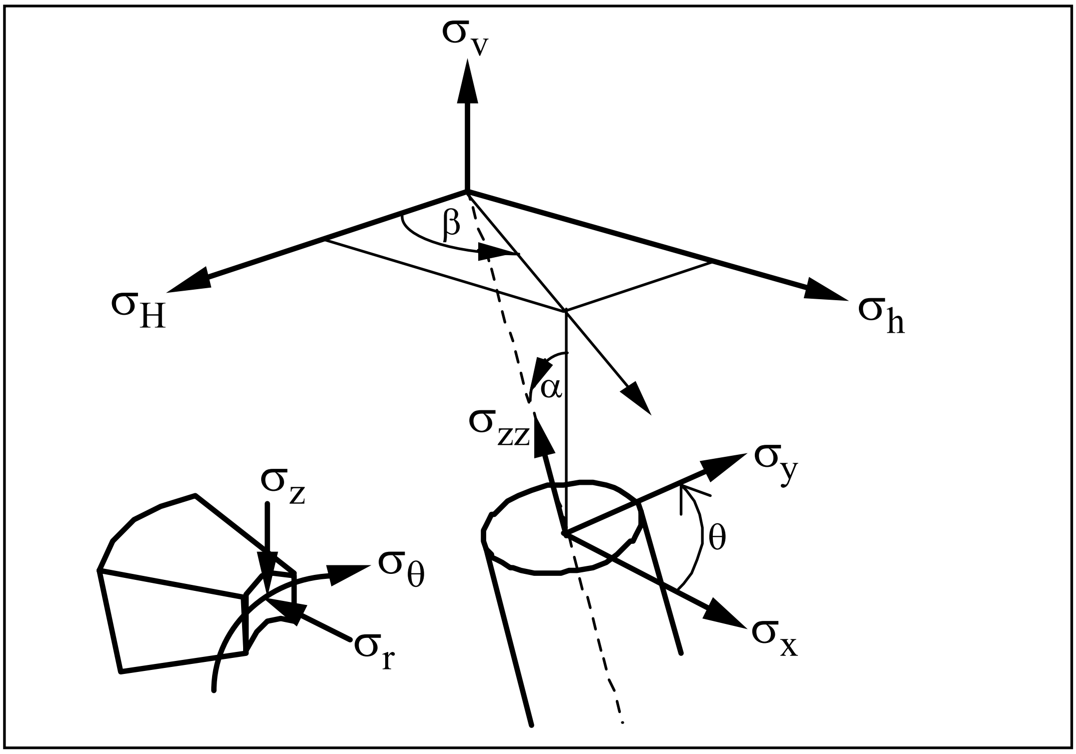

Fig. 1 Distribution of stresses acting on a deviated well [12].

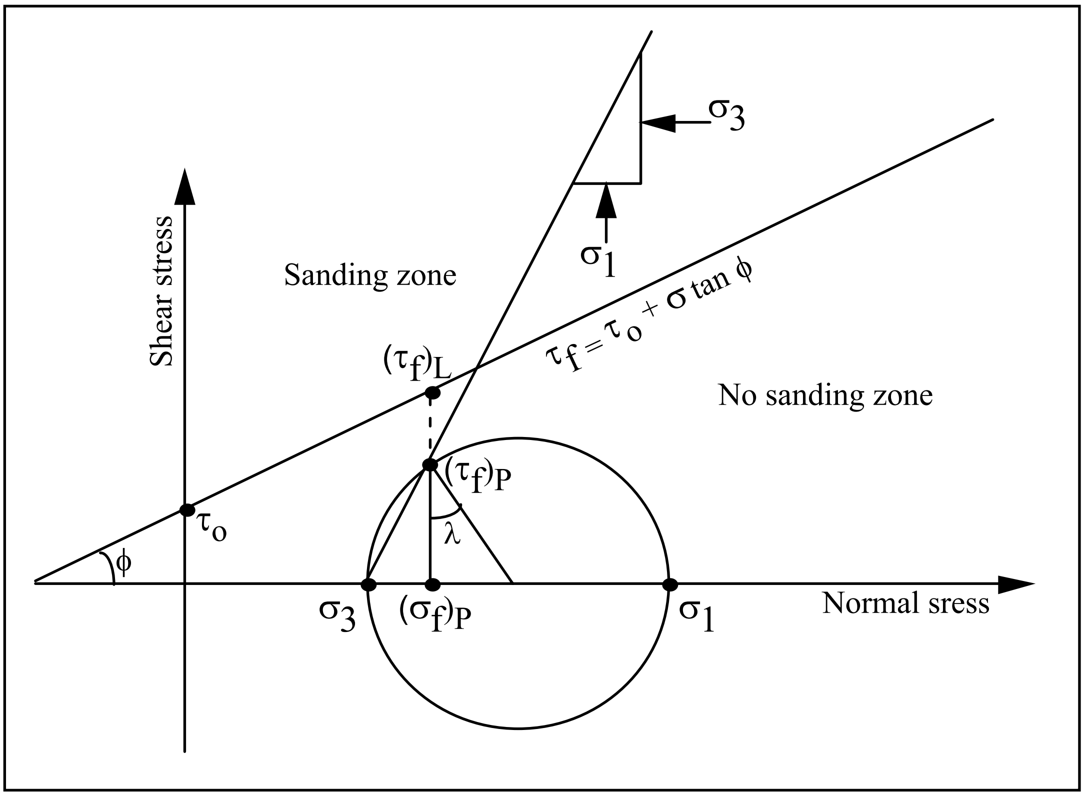

Fig. 2 The general case of Mohr-Coulomb failure criterion.

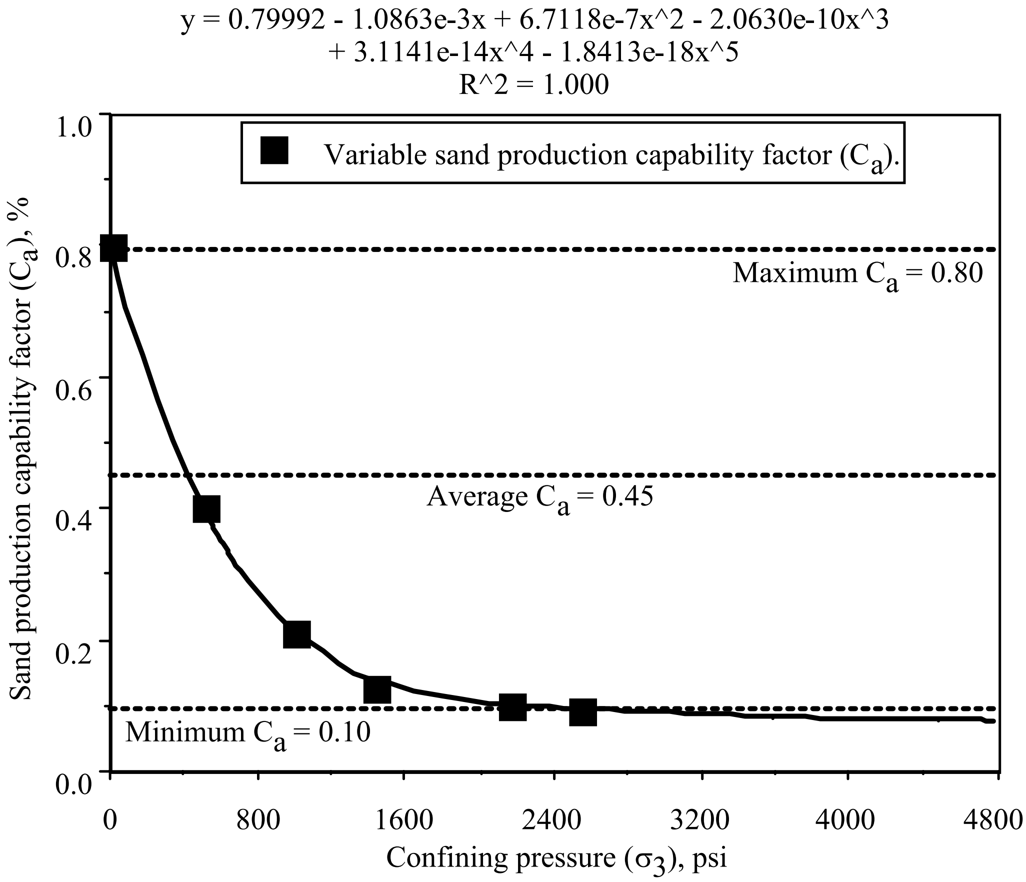

Fig. 3 Relationship between confining pressure and sand production capability factor for the studied reservoir.

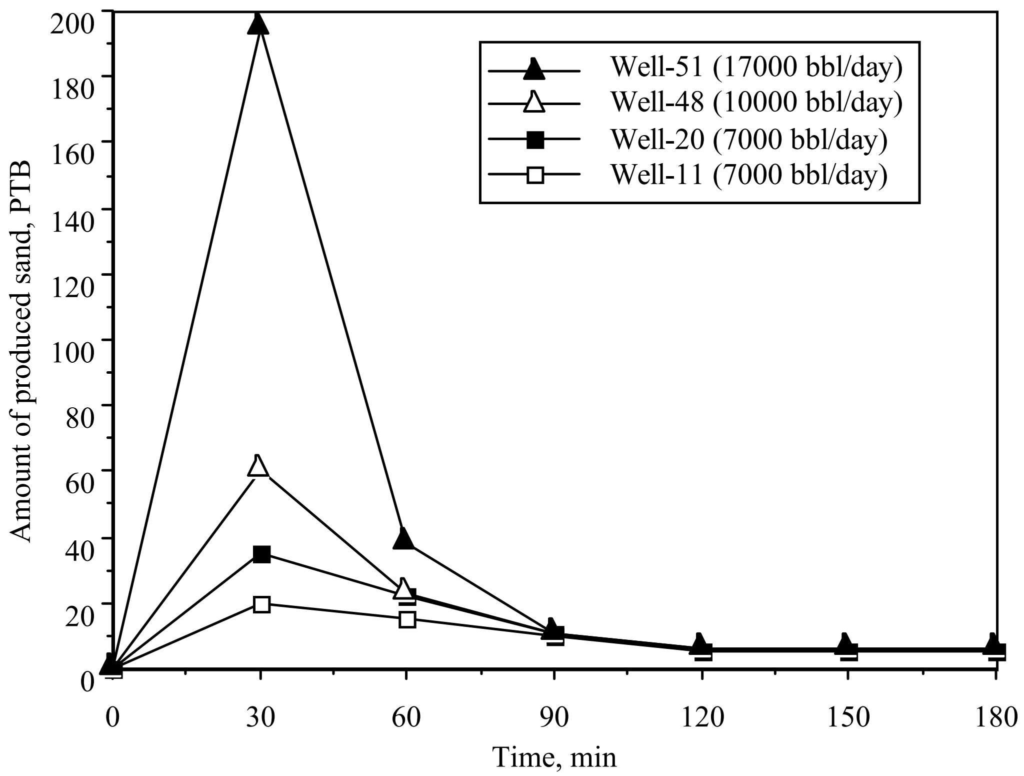

Fig. 4 Sand production trend for some Saudi oil reservoir wells [16].

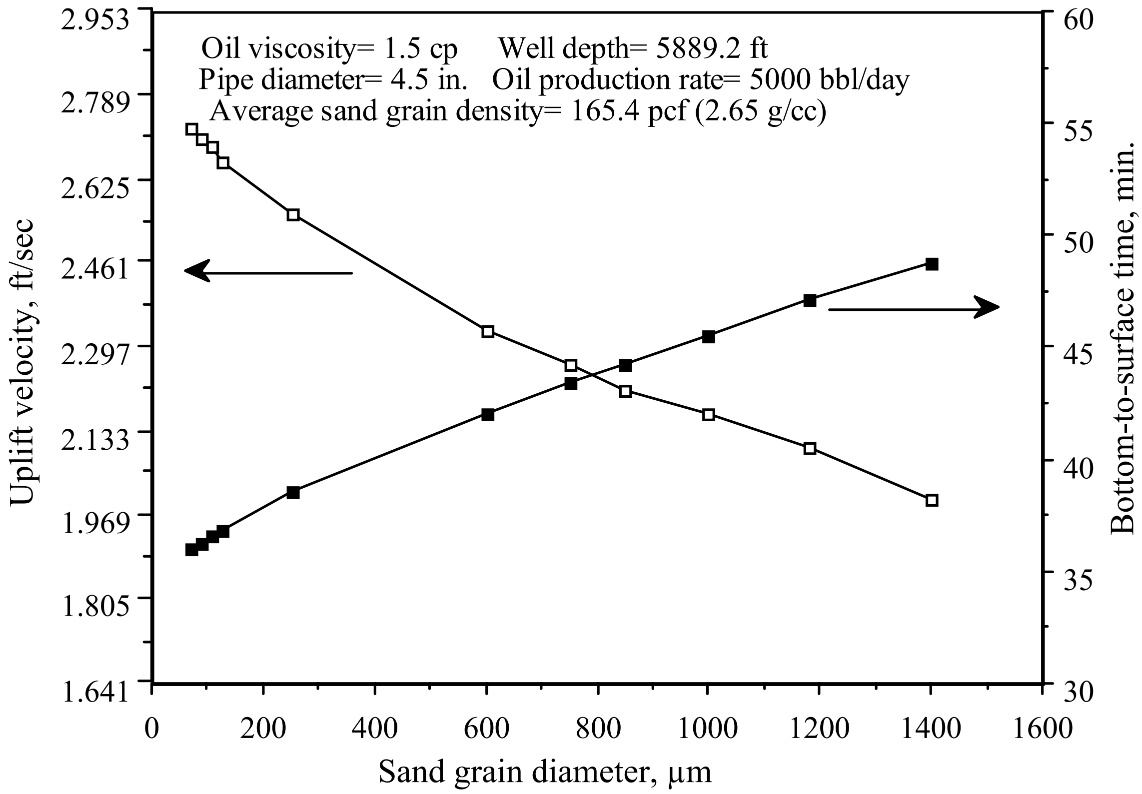

Fig. 5 Relationship between sand grain size, uplift velocity and bottom-to-surface time for the studied reservoir.

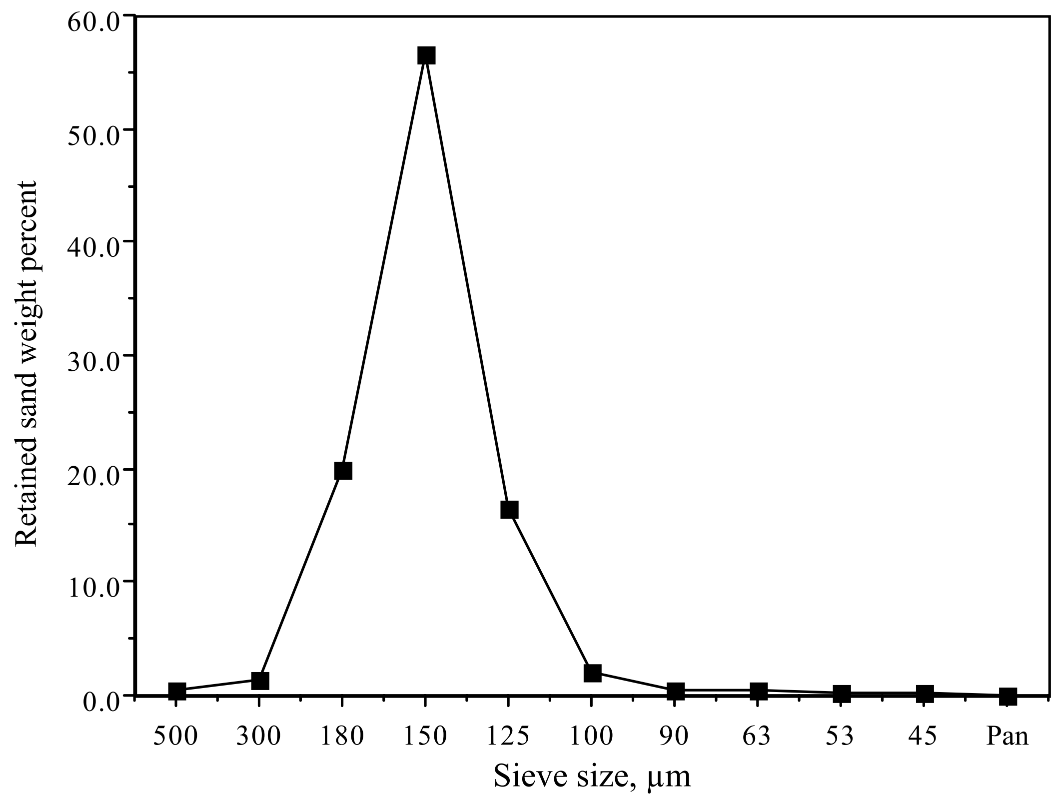

Fig. 6 Granulometric analysis of the studied reservoir.

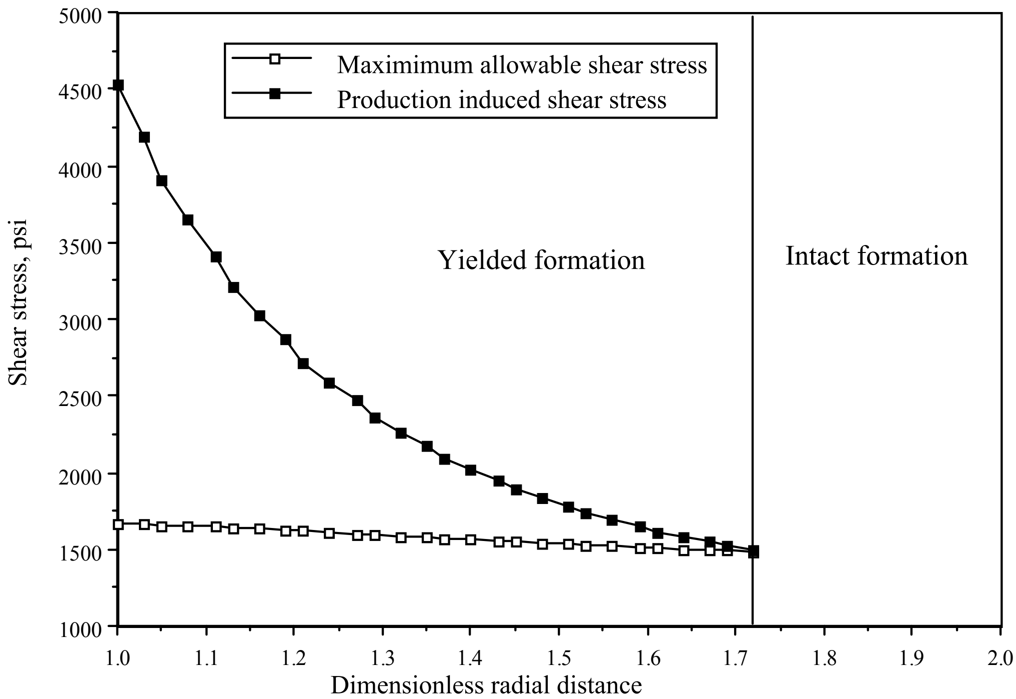

Fig. 7 Maximum shear stresses versus dimensionless radial distance for a vertical open-hole completed well in the studied reservoir.

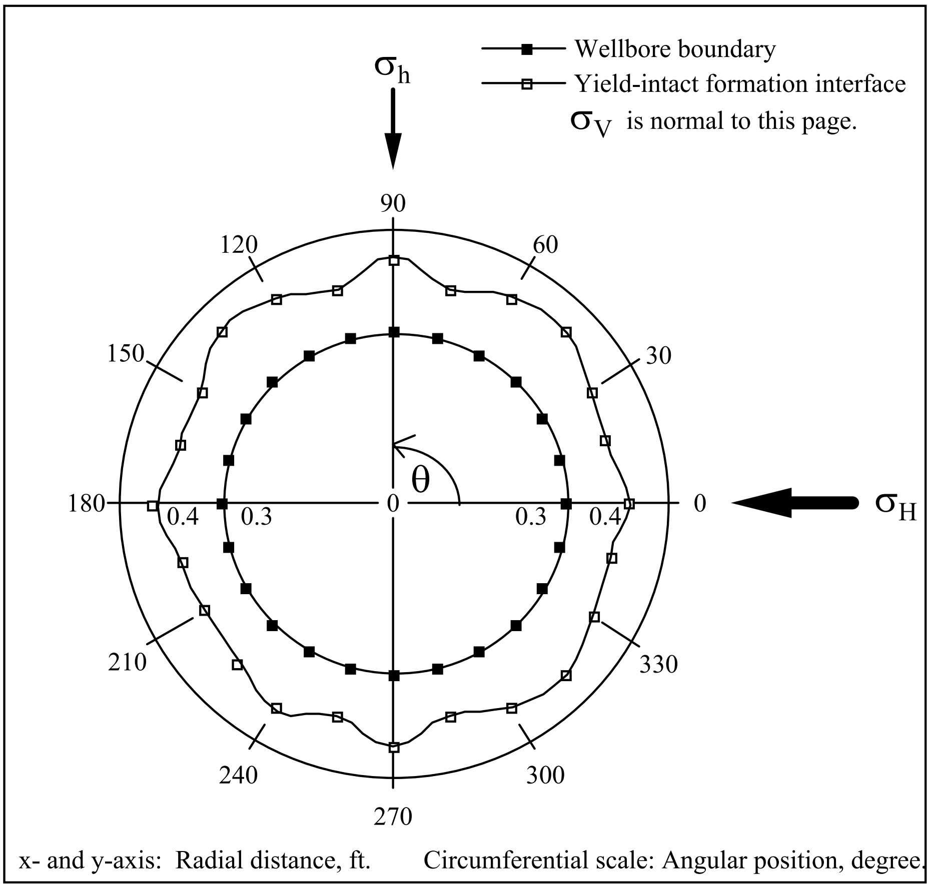

Fig. 8 Distribution of the yield zone around a vertical open-hole completed well in the studied reservoir producing at 5000 bbl/day.

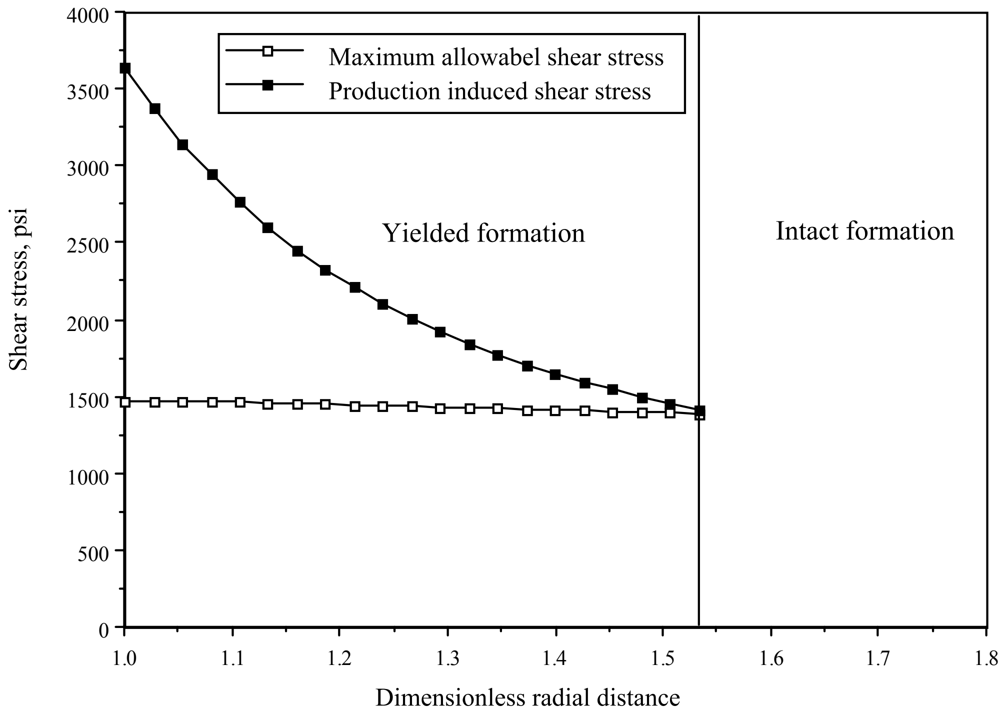

Fig. 9 Maximum shear stresses versus dimensionless radial distance for a horizzontal well in the studied reservoir (α=90°, β=0° and θ=0°).

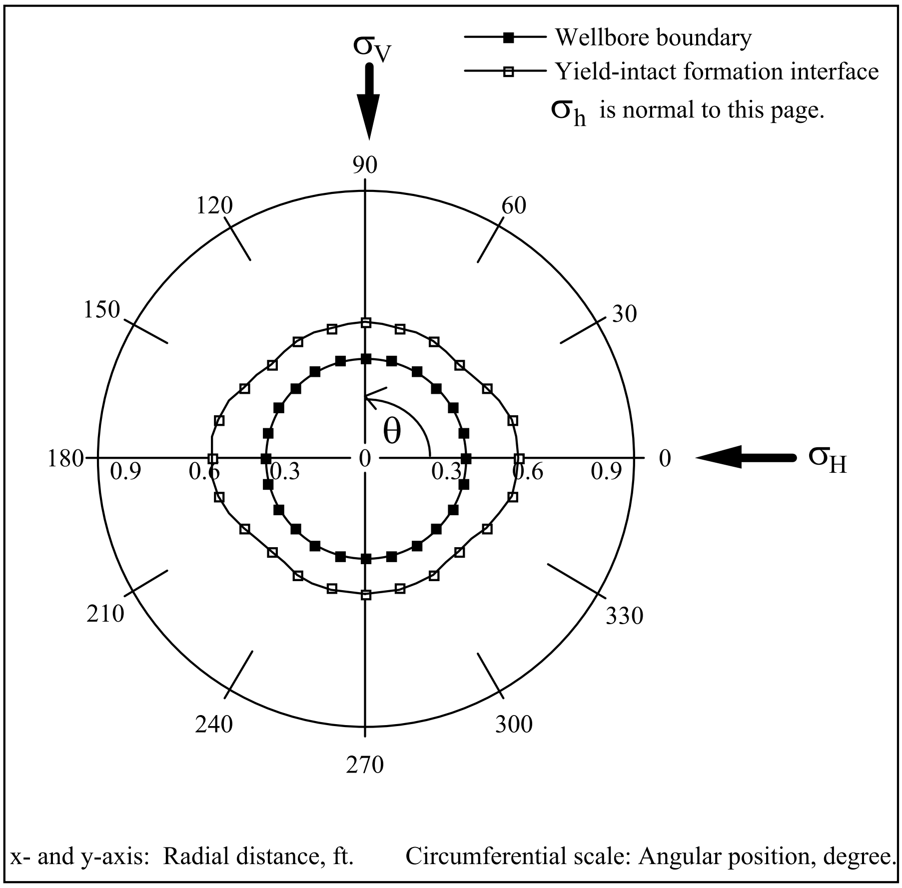

Fig. 10 Distribution of the yield zone around horizontal wells in the studied reservoir producing at 5000 bbl/day atβ= 0°.

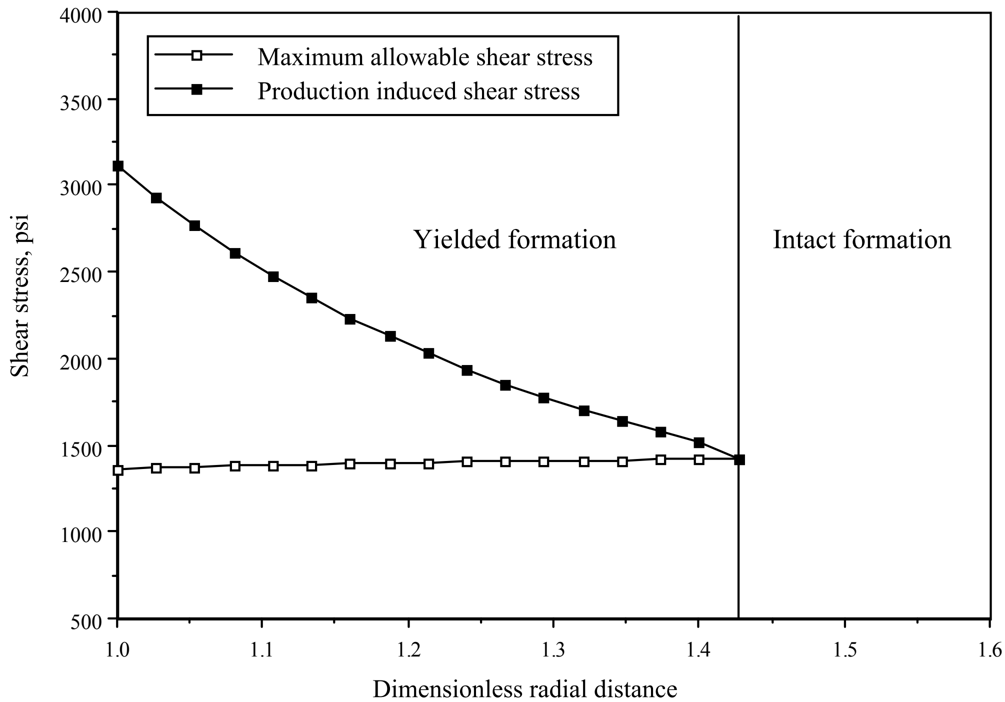

Fig. 11 Maximum shear stresses versus dimensionless radial distance for a horizontal well in the studied reservoir (α=90°, β=45° and θ=0°).

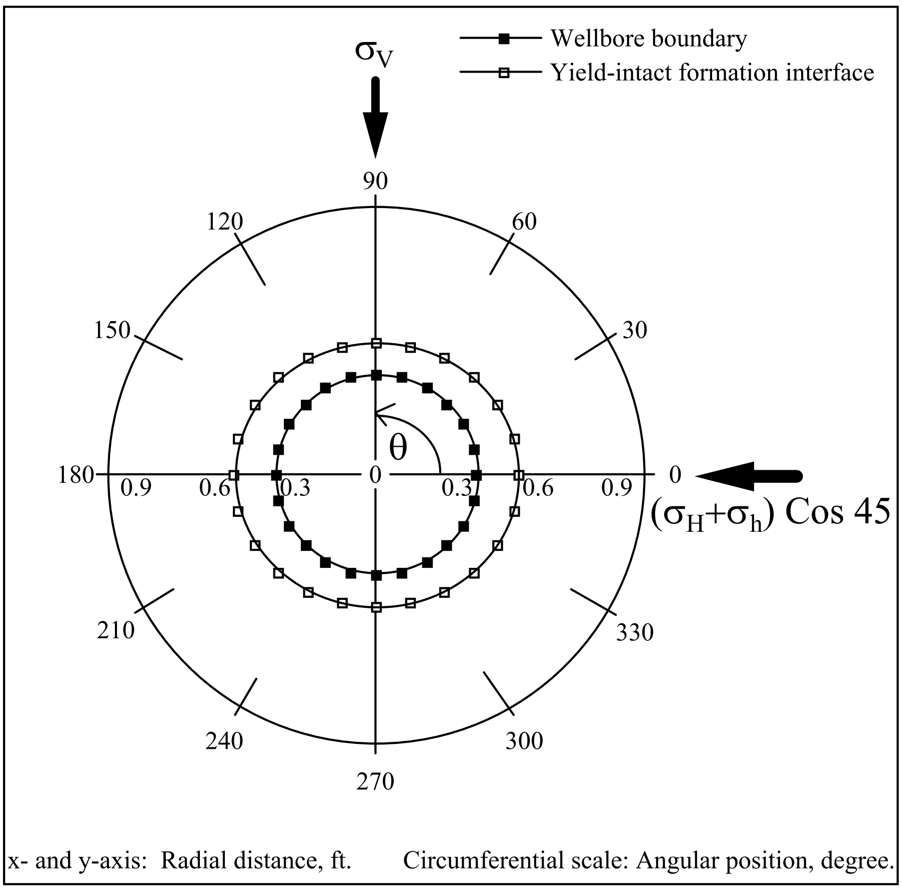

Fig. 12 Distribution of the yield zone around horizontal wells in the studied reservoir producing at 5000 bbl/day atβ = 45°.

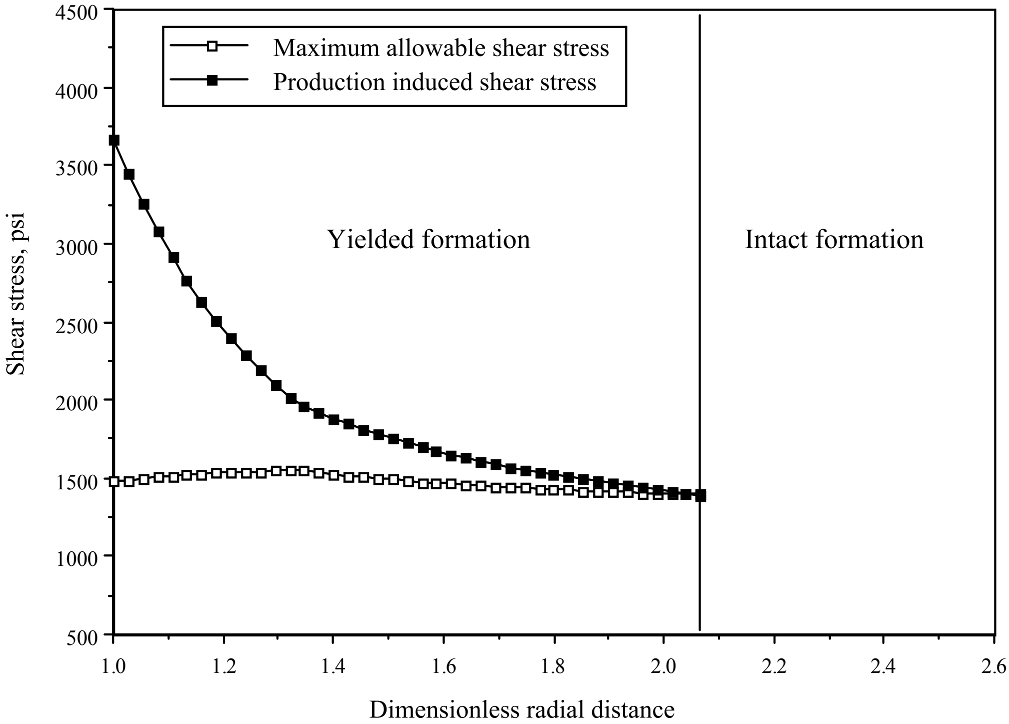

Fig. 13 Maximum shear stresses versus dimensionless radial distance for a horizontal well in the studied reservoir (α=90°, β=90° and θ=90°).

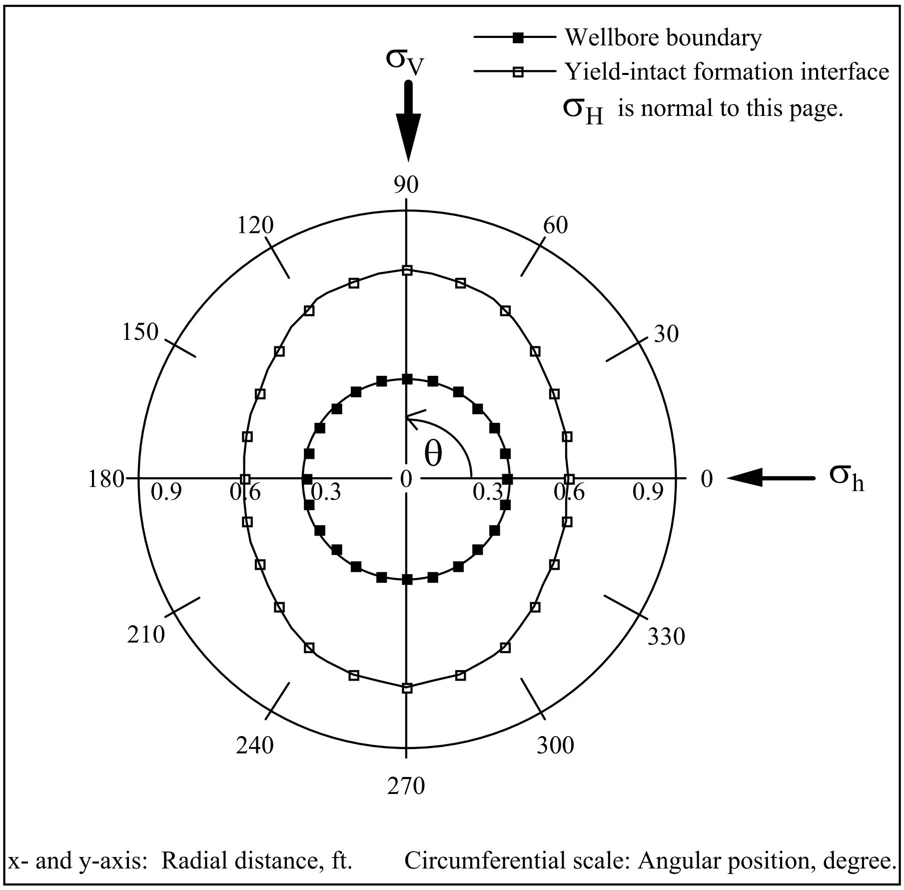

Fig. 14 Distribution of the yield zone around horizontal wells in the studied reservoir producing at 5000 bbl/day atβ= 90°.

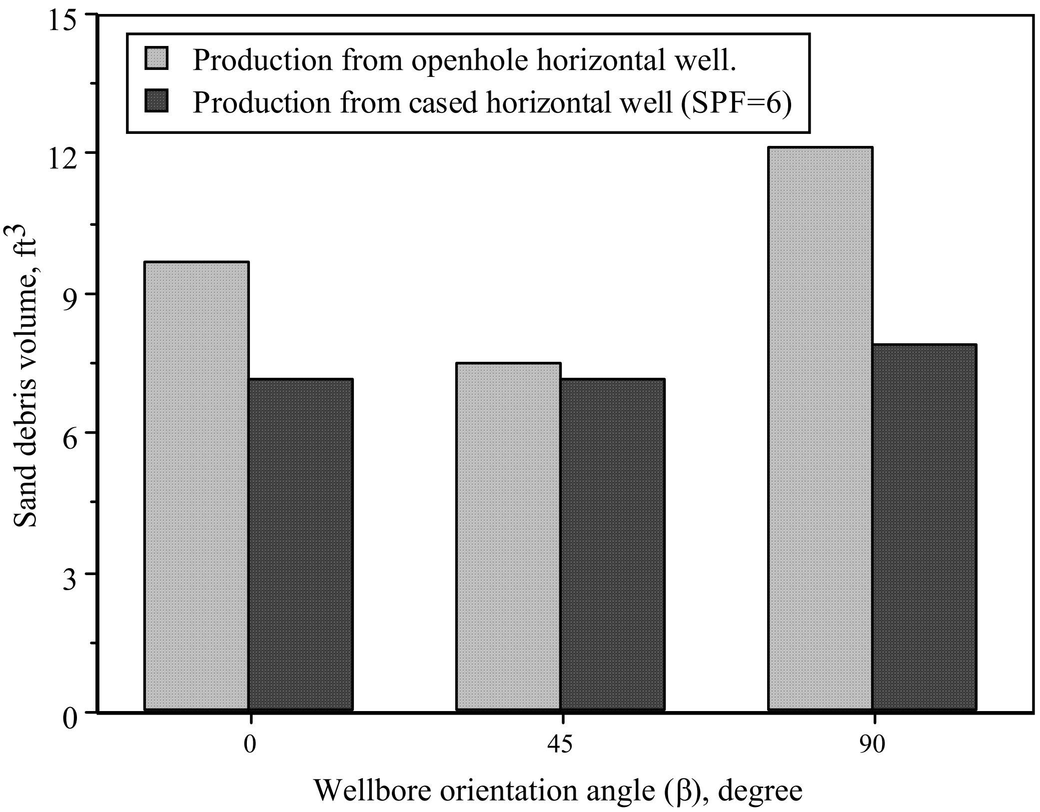

Fig. 15 Comparison between sand volumes gnerated in horizontal wells